HHS Public Access

Author manuscript

Oncogene. Author manuscript; available in PMC 2012 September 29.

Published in final edited form as:

Oncogene. 2012 March 29; 31(13): 1636–1648. doi:10.1038/onc.2011.346.

A role for caveolin-1 in desmoglein binding and desmosome dynamics

Donna Brennan, MS[1], **Sirkku Peltonen, MD, PhD**[2], **Alicia Dowling**[1], **Walid Medhat, MD**[1], **Kathleen J. Green, PhD**[3], **James K. Wahl III, PhD**[4], **Francesco Del Galdo, MD, PhD**[5], and **Mỹ G. Mahoney, PhD**[1,*]

[1]Department of Dermatology and Cutaneous Biology, Thomas Jefferson University, Philadelphia, PA, USA [2]Department of Dermatology, University of Turku and Turku University Hospital, Turku, Finland [3]Departments of Pathology and Dermatology, Northwestern University, Feinberg School of Medicine, Chicago, IL, USA [4]Department of Oral Biology, University of Nebraska Medical Center, Lincoln, Nebraska, USA [5]Scleroderma Research Centre, Leeds Institute of Molecular Medicine, University of Leeds, UK

Abstract

Desmoglein 2 (Dsg2) is a desmosomal cadherin that is aberrantly expressed in human skin carcinomas. In addition to its well-known role in mediating intercellular desmosomal adhesion, Dsg2 regulates mitogenic signaling that may promote cancer development and progression. However, the mechanisms by which Dsg2 activates these signaling pathways and the relative contribution of its signaling and adhesion functions in tumor progression are poorly understood. In this study we show that Dsg2 associates with caveolin-1 (Cav-1), the major protein of specialized membrane microdomains called caveolae, which functions in both membrane protein turnover and intracellular signaling. Sequence analysis revealed that Dsg2 contains a putative Cav-1 binding motif. A permeable competing peptide resembling the Cav-1 scaffolding domain bound to Dsg2, disrupted normal Dsg2 staining and interfered with the integrity of epithelial sheets *in vitro*. Additionally, we observed that Dsg2 is proteolytically processed; resulting in a 95 kDa ectodomain shed product and a 65 kDa membrane-spanning fragment, the latter of which localizes to lipid rafts along with full-length Dsg2. Disruption of lipid rafts shifted Dsg2 to the non-raft fractions, leading to the accumulation of these proteins. Interestingly, Dsg2 proteolytic products are elevated *in vivo* in skin tumors from transgenic mice overexpressing Dsg2. Collectively, these data are consistent with the possibility that accumulation of truncated Dsg2 protein interferes with desmosome assembly and/or maintenance to disrupt cell-cell adhesion. Furthermore, the association of Dsg2 with Cav-1 may provide a mechanism for regulating mitogenic signaling and modulating the cell surface presentation of an important adhesion molecule, both of which could contribute to malignant transformation and tumor progression.

*Address for Correspondence: Mỹ G. Mahoney, Ph.D., Department of Dermatology and Cutaneous Biology, Jefferson Medical College, 233 S. 10th Street, Suite 428 BLSB, Philadelphia, PA 19107, Tel: 215-503-3240, Fax: 215-503-5788, my.mahoney@jefferson.edu.

Conflict of Interest: The authors declare no conflict of interest

Keywords

Carcinogenesis; Caveolin; Caveolae; Desmoglein; Keratinocyte

Introduction

Desmogleins are the major transmembrane proteins of the cell-cell adhesion structures known as desmosomes. There are four distinct desmoglein genes (Dsg1-4) in humans, which are expressed in a tissue-type and differentiation-specific manner (Cheng and Koch, 2004; Garrod et al., 2002; Mahoney et al., 2006). Studies involving *Dsg2* null mice revealed that Dsg2 contributes to embryonic stem cell proliferation, particularly in the inner cell mass of the developing blastocyst (Eshkind et al., 2002). Dsg2 is aberrantly expressed in select epithelial malignancies, including squamous cell carcinomas (Biedermann et al., 2005; Harada et al., 1996; Kurzen et al., 2003). Similarly, genetic profiling of prostate cancer cell lines showed increased expression of Dsg2 in a metastatic cell line, as compared to its non-metastatic syngeneic precursor cell (Trojan et al., 2005). Dsg2 expression is also upregulated in squamous cell carcinoma (SCC) cell lines in comparison to cultured keratinocytes (Denning et al., 1998; Harada et al., 1996; Schäfer et al., 1994). We recently showed that Dsg2 is highly expressed in malignant skin carcinomas, including squamous cell carcinomas, basal cell carcinomas, sweat and sebaceous gland carcinomas and adenocarcinomas (Brennan and Mahoney, 2009). Collectively, these results support a role for Dsg2 in epithelial cell growth, survival and malignant transformation. However, the mechanisms by which Dsg2 activates these signaling pathways and promotes tumor formation are unknown.

Caveolins are a family of hairpin-like, palmitoylated, integral membrane proteins that oligomerize and bind to cholesterols and sphingolipids to form specialized areas of the membrane distinct from the clathrin-coated pits. The caveolins form flask-shaped invaginations of 50-100 nm in diameter called caveolae (Severs, 1988). There are three caveolin isoforms: Cav-1 (α and β), Cav-2 and Cav-3. While Cav-1 and Cav-2 are ubiquitously expressed, Cav-3 expression is predominantly restricted to muscle cells (Scherer et al., 1995; Tang et al., 1996). Caveolins and caveolae have been implicated as regulators of key cellular functions, including cholesterol transport and homeostasis (Fielding and Fielding, 1995; Smart et al., 1996), endocytosis and endocytic vesicle trafficking (Schnitzer and Oh, 1996), cell adhesion and apoptosis (Kurzchalia and Parton, 1999; Lisanti et al., 1994; Okamoto, 1998; Okamoto et al., 1998; Shaul and Anderson, 1998). Specific cell signals can be also transmitted through a spatially controlled organization of cell receptors into the caveolae. Indeed, the epidermal growth factor (EGF) receptor has been shown to stimulate the phosphorylation of Cav-1, thus enhancing caveolae assembly (Orlichenko et al., 2006; Severs, 1988; Simons and Toomre, 2000; Singer and Nicolson, 1972). Furthermore, Cav-1 is essential for integrin-mediated activation of PI3-K/AKT (Sedding et al., 2005). Conversely, overexpression of Cav-1 abrogates anchorage-independent cell survival (Engelman et al., 1997), and suppresses cell growth (Lee et al., 1998). Additionally, Cav-1 binds to and inhibits kinases involved in mitogenic signaling pathways. Cav-1 expression can modulate Wnt/β-catenin/Lef-1 signaling by regulating the

intracellular localization of β-catenin (Galbiati et al., 2000). Consistent with these findings, mounting evidence suggests that diseases associated with deregulated signaling pathways often result from aberrant expression or localization of Cav-1. In cancer, the role for Cav-1 is complex, as it serves both as a modulator of tumor suppression as well as oncogenesis. Mutations in the *Cav-1* gene have been linked to human breast cancer, suggesting that loss of Cav-1 function plays a significant role in tumor initiation (Chen et al., 2004). Mice devoid of Cav-1 develop mammary epithelial cell hyperplasia (Capozza et al., 2003) and are susceptible towards mammary tumorigenesis (Park et al., 2002). In the skin, *Cav-1* null mice are also more susceptible to epidermal hyperplasia and skin tumor formation in response to carcinogens (Capozza et al., 2003).

In this report, we provide strong evidence that Dsg2 interacts directly with Cav-1, and that these interactions may impact Dsg2 recycling, desmosome dynamics and cell adhesion; and furthermore, provide a mechanism by which Dsg2 mediates cell signaling.

Results

Co-localization of Cav-1 and Dsg2

We recently showed that over-expression of Dsg2 in the epidermis results in hyperproliferation and the formation of pre-cancerous papillomas; additionally, Dsg2 transgenic mice are more susceptible to chemical-induced skin carcinogenesis (Brennan et al., 2007). Furthermore, Dsg2 overexpression in the skin of these mice results in activation of several signaling pathways directly relevant to epithelial cell proliferation and survival, notably the PI-3-kinase/AKT, MEK/MAPK and NF-κB pathways. We thus searched for Dsg2 binding partners that could interact with the intracellular domain, and potentially lead to the activation of downstream signaling events. We generated glutathione S-transferase (GST) fusion recombinant proteins of the intracellular domains (cytoplasmic tails) of Dsg1 and Dsg2. The GST fusion proteins were affinity-purified using glutathione sepharose beads, and bound proteins were eluted with glutathione elution buffer according to the manufacturer's protocol (Figure 1A). To confirm the identity of the fusion proteins, we performed Western blotting analysis using the antibodies H-145 and DG3.10 (Figure 1B). We note here that there are two commercially available H-145 antibodies; one recognizes Dsg2 while the other, Dsg3. Throughout this report, we used the Dsg2 H-145. Antibody DG3.10 recognizes both Dsg1 and Dsg2. Immunoblot analysis showed that H-145 recognized only the GST-Dsg2.tail, while DG3.10 detected both GST-Dsg1.tail and the GST-Dsg2.tail.

The GST fusion proteins were used to affinity purify proteins from A431 cell lysates. By Western blot analysis, we first demonstrated that the desmosomal protein γ-catenin (plakoglobin), but not the adherens junction protein β-catenin, was able to bind to Dsg1 and Dsg2 (Figure 1C). It was previously demonstrated that Dsg3 localizes to lipid rafts (Delva et al., 2008) and here we identified Cav-1 as one of several novel Dsg2-binding proteins. Western blotting of cellular proteins eluted from the columns demonstrated that Cav-1 (22 kDa) interacted with Dsg2 and Dsg1, but not GST alone (Figure 1D).

Next, we performed immunoprecipitation assays to confirm the Dsg2-Cav-1 interaction. A431 cells were extracted into detergent free and Triton X-100 (Tx)-containing protein fractions, incubated with antibody 10D2 (Keim et al., 2008), and the Dsg2 immunocomplexes were pulled down with protein A/G. The precipitated products were immunoblotted with H-145, to confirm the pull-down of the 160 kDa Dsg2 in the Tx-fraction (Figure 1E). Cav-1 was detected in both detergent free and Tx-containing fractions. However, the detergent free fraction showed higher levels of Cav-1, suggesting perhaps that, while Cav-1 associated with both desmosome-bound and desmosome-free Dsg2, it was more likely to associate with Dsg2 outside of the desmosomal structure, i.e., in lipid rafts. In summary, these results demonstrate that full-length Dsg2 binds to Cav-1.

To confirm Dsg2-Cav-1 co-localization at the cell level, we performed double-labeled immunofluorescence and laser scanning confocal microscopy for Dsg2 (green) and Cav-1 (red) in A431 cells (Figure 2). We did not expect to see extensive co-localization of Dsg2 and Cav-1 since desmogleins are predominantly found in desmosomes and Cav-1 in lipid rafts. Indeed, we observed the hallmark punctate cell-cell border pattern for Dsg2, while Cav-1 had diffuse cytoplasmic and cell surface staining pattern. However, consistent with our immunoprecipitation results above, we did observe some co-localization of Dsg2 with Cav-1 at the membrane.

Next, we wanted to determine whether Cav-1 and desmogleins are expressed in similar cell compartments in normal human epidermis. We performed co-localization experiments for Cav-1 and Dsg1/Dsg2 (Figure S1). We observed pronounced Cav-1 staining at the cell-cell borders, as well as in the cytoplasm of keratinocytes in the basal and the immediate suprabasal layers, which is in accordance with the literature (Gassmann and Werner, 2000). In the same epidermal layers, we observed strong staining of Dsg1 and Dsg2 using antibody DG3.10. Merged image showed some co-localization, particularly at the cell-cell borders (arrows demarcate co-localization). These results demonstrate that, in human skin, Cav-1 is expressed in the basal and most immediate suprabasal epidermal layers where desmogleins could be found. Thus, consistent with our immunoprecipitation results above, we observed co-localization of desmogleins with Cav-1 primarily at the plasma membrane. In the hair follicle, where both Dsg2 and Cav-1 expression levels were high, we observed strong staining of both Dsg2 and Cav-1 in cells of the outer root sheath (not shown).

Dsg2 interacts with Cav-1 through the Dsg2 consensus-binding motif and the Cav-1 scaffolding domain

Cav-1 association with many protein-binding partners is mediated by a conserved 20-amino acid domain called the caveolin-scaffolding domain (CSD), located between Asp82 and Arg101 (DGIWKASFTTFTVTKYWFYR) of Cav-1. This conserved domain binds several consensus-binding motifs (φXφXXXXφ, φXXXXφXXφ and φXφXXXXφXXφ; where φ are aromatic amino acids phenylalanine F, tyrosine Y and tryptophan W) present on signaling molecules (Lisanti et al., 1994; Okamoto et al., 1998). In some cases, hydrophobic amino acids are found in the place of aromatic amino acids, and the binding motifs may also be reversed in orientation (φXXXXφXφ, φXXXXφXXφ, or φXXφXXXXφXφ). Examination of the Dsg2 amino acid sequence revealed a potential Cav-1 binding motif

($_{776}$FTDKAASY$_{783}$) in the cytoplasmic tail domain (Mahoney et al., 2002; Whittock, 2003) (Figure 3A). To demonstrate that Dsg2 can associate with the Cav-1 scaffolding domain, we generated a fusion peptide consisting of the *Drosophila* Antennapedia (AP, RQPKIWFPNRRKPWKK) homeodomain, and a putative competing peptide resembling the scaffolding domain of Cav-1. The AP and AP-Cav-1 peptides are cell-permeable and are biotinylated at the amino terminus (Figure 3B). The bioactive Cav-1 fragment, AP-Cav-1, was previously used to restore Cav-1 bioavailability and abrogate TGF-beta activation of cultured human dermal fibroblasts (Del Galdo *et al.*, 2008). For our study, we reasoned that the peptide would disrupt the binding of Dsg2 with Cav-1. Thus, we treated A431 cells with either AP or AP-Cav-1 (5 μM) in serum-free medium for 1 hr, and lysed in a 1% Tx lysis buffer. Cell lysates were incubated with anti-Dsg2 antibody 10D2 and precipitated with Protein A/G Agarose. Precipitated proteins were resolved by SDS-PAGE and immunoblotted with Strep Avidin-HRP (Figure 3C). The results showed that anti-Dsg2 pulled down biotinylated AP-Cav-1, but not biotinylated AP alone. These results demonstrate that Dsg2 associates with Cav-1, most likely through the Cav-1 scaffolding domain.

To further assess whether Cav-1 plays a role in maintaining desmosome dynamics, we treated A431 cells with the peptides AP and AP-Cav-1 for 24 hrs. Cells were then fixed and immunostained for Dsg2 using 6D8 or DG3.10 (Figure 4). Dsg2 was detected at the cell-cell border in cells treated with DMSO or AP peptide. However, treatment with AP-Cav-1 peptides dramatically altered the localization of Dsg2 (Figure 4). We observed diffuse cell surface staining with loss of the hallmark punctate cell-cell border staining. We note here that the haziness of the stainings of the AP-Cav-1 treated cells is consistent throughout our experiments with the use of this AP-Cav-1 peptide, and is not due to errors in photography. In summary, our results thus far demonstrate that Cav-1 binds to Dsg2, most likely through the Cav-1 binding domain. Disrupting Cav-1 binding with competing peptides results in profound changes in cell surface localization of Dsg2. We note here that although it is well established that caveolins localize to caveolae, structures that are defined by electron microscopy, since we did not utilize electron microscopy in this study, we will refer to these structures as lipid rafts or membrane microdomains.

Co-localization of Dsg2 to membrane microdomains

To further confirm that Dsg2 binds to Cav-1, and to determine whether Dsg2 co-localizes with Cav-1 in lipid-enriched rafts, we performed sucrose-density-gradient fractionation. Lipid rafts are discrete specialized plasma membrane microdomains (Brown and London, 1998; Simons and Ikonen, 1997). Due to their high cholesterol and sphingolipid content, they can be isolated based on their detergent-insolubility and/or low-buoyant density (detergent-free fractionation). We used 5-35% discontinuous sucrose gradient ultracentrifugation to isolate caveolin-rich membrane microdomains from A431 cells as previously described (Galbiati et al., 2000; Song and Dohlman, 1996; Zheng et al., 2003). Proteins exhibit a light buoyant density because they are encased in ‘lipid shells’ of cholesterol and sphingolipids (Wang et al., 2003). We observed both Dsg2 and Cav-1 localized to lighter gradient fractions of 4-5 (Figure 5A). In addition to Cav-1 and Cav-2, we detected other lipid raft proteins, including flotillins (Flo1 and Flo2). Additionally, we also

detected the desmoglein-associated protein, plakoglobin (γ-catenin), in the lipid raft fractions. Proteins of the adherens junction did not co-fractionate under these conditions, and were primarily in the more dense fractions. Both E-cadherin and β-catenin were detected in fractions 6-12. Low levels of β-catenin were also detected in fractions 4 and 5. Interestingly, Dsg2 appeared evenly distributed throughout all sucrose fractions. We posit that Dsg2 may associate with other caveolae-free membrane microdomains such as low density, Triton-resistant, and glycospingolipid-enriched membrane domains (Fra et al., 1994). However as mentioned above, without using electron microscopy we cannot conclusively ascertain whether Dsg2 resides in caveolae or simply in microdomains similar to caveolae.

Methyl β cyclodextran (MβCD) and filipin are two widely accepted treatments for manipulating cholesterol-containing domains. Disruption of lipid rafts with MβCD results in the loss of compartmentalization and caveolae formation, and shifts Cav-1 out of lipid rafts and into denser gradient fractions (Furuchi and Anderson, 1998). Here, we observed a shift of both Cav-1 and Dsg2 into the higher density fractions 11 and 12 with MβCD treatment (Figure 5A, right panels). A shift in density fractionation was also observed with Cav-2, Flo1 and Flo2 and γ-catenin. On the other hand, MβCD did not alter the distribution β-catenin, E-cadherin and actin; they all still localized mainly to the non-lipid raft fractions. Similar results, although to a lesser extent, were observed when cells were treated with filipin (data not shown), which also binds to cholesterol and alters membrane permeability (Laughlin et al., 2004).

Interestingly, in untreated control cells, we observed a band of weaker intensity at approximately 65 kDa that was recognized by the Dsg2 antibody in fraction #4 (Figure 5A, vertical arrow). Treatment with MβCD resulted in an accumulation of this 65 kDa fragment (Fig. 5A, arrow head), which was shifted to the high-density fractions along with the full length 160 kDa Dsg2 (arrow). To further characterize the 65 kDa Dsg2 fragment, proteins from sucrose gradient fractions #4 and #12 of cells both untreated and treated with MβCD were resolved over SDS-PAGE and immunoblotted with Dsg2 antibodies 10D2 and DG3.10 (Figure 5B). Antibody 10D2, which recognizes the extracellular domain 1 (EC1) of Dsg2 (Brennan and Mahoney, 2009; Keim et al., 2008), detected only the 160 kDa full-length Dsg2 band in both fractions #4 and #12. Antibody DG3.10, which recognizes epitopes within the intracellular domain of Dsg2, recognized both the full-length protein and the truncated 65 kDa fragment (arrowhead). The antigenic epitopes of these antibodies have been previously characterized in detail (Brennan and Mahoney, 2009). Thus, our data demonstrates that the 160 kDa full-length and the truncated 65 kDa intracellular fragment both localized to lipid rafts. Disruption of lipid rafts led to the retention of the 65 kDa intracellular domain of Dsg2 in the non-lipid raft membrane fractions.

Next, we wanted to assess whether treatment with MβCD would alter subcellular localization of Dsg2. Cells were fixed and stained for Dsg2 (antibody DG3.10) and Cav-1 (Figure 6). In control untreated cells, we observed diffuse cell surface staining for Cav-1 (panel a; red) and punctate cell-cell border staining for Dsg2 (panel b; green). In response to MβCD treatment, we observed detachment of keratinocytes and enhanced localization of Cav-1 to the cytoplasm (panel e). Interestingly, treatment with MβCD also resulted in an

increase in cytoplasmic staining for Dsg2. MβCD had little effect on the cell-cell border localization of Dsg2, however the cell-cell contacts were no longer contiguous. Interestingly, at the points of cell-cell contacts, we observed an increase in co-localization of Dsg2 and Cav-1. We surmise that the treatment with MβCD disrupted caveolae formation thereby releasing Cav-1 from these specialized membrane rafts. Cav-1 may then freely associate with other desmogleins or junctional proteins.

Disruption of Cav-1 association altered Dsg2 localization and keratinocyte cell adhesion

Next, we wanted determine whether disrupting the Dsg2-Cav-1 interaction would alter Dsg2 localization within lipid rafts by examining the effect of AP-Cav-1 on Dsg2 distribution in light versus heavy membrane fractions following sucrose gradient fractionation. A431 cells were treated with AP and AP-Cav-1 peptides (5 μM) for 2 hr. Total cellular proteins were separated over a discontinous sucrose-gradient. Fractionated proteins were resolved over SDS-PAGE and immunoblotted for Dsg2 and Actin (supplemental Figure S2). Disrupting the interaction between Dsg2 and Cav-1 with the Cav-1 competing antennapedia peptides partially shifted Dsg2 out of the low-density membrane lipid raft fractions. Furthermore, the Cav-1 competing peptides also induced loss of keratinocyte adhesion. After treating A431 cells with AP or AP-Cav-1 peptides, cells were dislodged from the petri dish using dispase. Cell sheets were subjected to dispase-based keratinocyte dissociation assay showing more fragmentation after treatment with AP-Cav-1 peptides, as compared to control untreated or treated with AP alone. Shown are representative results from three separate experiments (supplemental Figure S3).

Proteolytic processing of Dsg2 during malignant transformation

It was previously demonstrated that shedding of the extracellular domain of Dsg2 protects epithelial cells from apoptosis (Nava et al., 2007). To determine whether the 65 kDa Dsg2 fragment observed here resulted from ectodomain shedding, we collected conditioned media from various epithelial-derived cell lines and performed immunoblot analysis to detect the shed fragment of Dsg2. Of the cell lines tested, the JAR choriocarcinoma cell line showed the highest level of Dsg2 expression (Figure 7A). Cells were then grown to confluency and the conditioned medium was collected, concentrated and immunoblotted for Dsg2. The results showed a shed ectodomain product of approximately 95 kDa (barbed arrow), detected by 10D2, but not DG3.10 (Figure 7B, lanes M for medium). Tx-soluble and -insoluble fractions were prepared from JAR cells and immunoblot analysis revealed a 65 kDa fragment recognized by DG3.10, but not 10D2 (Figure 7B, arrowhead).

Since A431 cells showed significantly less Dsg2 cleavage as compared to JAR cells, we treated A431 cells with the cytotoxic quinoline alkaloid camptothecin (10 μM) for 6 hrs to induce apoptosis and processing of many proteins. Supernatant was collected, concentrated and proteins were immunoblotted with a series of antibodies against the extracellular (10D2, 10G11, Rb5, 6D8, and Ab10) and cytoplasmic (H-145 and DG3.10) domain of Dsg2 (Figure 7C). Treatment with camptothecin enhanced ectodomain shedding of Dsg2, resulting in an accumulation of the 95 kDa fragment, which was recognized by antibodies to the extracellular domain but not antibodies to the intracellular domain (Figure 7C, barbed

arrow). We note that the more sensitive Dsg2 antibodies, 6D8 and Ab10, detected some shed Dsg2 in the medium of control untreated cells.

To determine whether the 65 kDa Dsg2 fragment binds to Cav-1, we performed immunoprecipitation followed by Western blotting analysis. Camptothecin-treated A431 cell lysate was immunoprecipitated with Cav-1 antibodies, and the precipitated product was immunoblotted with antibodies Ab10 and H-145 (Figure 7D). We note here that antibody Ab10 was raised against extracellular domain 5 (EC5) of Dsg2, the region adjacent to the transmembrane domain (Brennan and Mahoney, 2009). Ab10 recognized both the 95 kDa extracellular shed product as well as the 65 kDa membrane-spanning fragment (not shown). Immunoblots performed with Ab10 and H-145 detected a band migrating at approximately 65 kDa after precipitation for Cav-1. These findings further support our results above that the 65 kDa Dsg2 fragment associates with Cav-1. Our data thus far demonstrate that both the full-length 160 kDa and the truncated 65 kDa intracellular fragment localize to lipid rafts, and interact with Cav-1. Furthermore, although Cav-1 can bind to the full-length protein, it binds predominantly to the 65 kDa fragment. Disruption of lipid rafts may lead to re-localization of this truncated 65 kDa product.

Finally, we wanted to determine if Dsg2 undergoes proteolytic processing during skin cancer development, *in vivo*. For these experiments, we used a transgenic mouse line that was recently established in our laboratory, where Flag-tagged Dsg2 is expressed under control of the involucrin promoter (Brennan et al., 2007). Inv-Dsg2 transgenic and wild type control littermates were subjected to DMBA (7,12-dimethylbenz-alpha-anthracene)/TPA (12-*O*-tetradecanoylphorbol 13-acetate)-induced skin tumor development as previously described for 8 weeks (Brennan et al., 2007). Skin tumor tissues were extracted in Laemmli sample buffer, proteins were resolved by SDS-PAGE and immunoblotted using polyclonal anti-Flag antibody. We detected the 160 kDa Dsg2-Flag protein in the skin and tumors from transgenic, but not in wild type mice (Figure 8A, arrow). Interestingly, although the level of full-length Dsg2 in the tumors of transgenic mice was comparable to unaffected skin in these mice, the level of proteolytic processing of Dsg2 protein was significantly enhanced in the tumor tissues. Amongst the many unique bands ranging from the 160 kDa full-length Dsg2 protein to a small 40 kDa fragment detected by the Flag antibody, we observed a major band of approximately 65 kDa (Figure 8A, arrow head).

Several older Inv-Dsg2 transgenic mice developed spontaneous skin tumors (not shown). Thus far, none of the wild-type littermates have developed tumors, as expected of the tumor-resistant C57Bl6 background. To further confirm the proteolytic processing of Dsg2 in tumor tissues, we extracted proteins from spontaneously derived tumors and tumors derived after DMBA/TPA treatment. Again, proteins were resolved over SDS-PAGE for Western blotting, but this time, using a monoclonal anti-Flag antibody (Figure 8B). Immunoblots showed that, in addition to the 160 kDa full-length protein (arrow), we observed a prominent 65 kDa band (arrow head). Thus, we propose that the 65 kDa band observed here maybe the membrane-spanning intracellular Dsg2 product resulting from ectodomain shedding, and that generation of this product may play a role in tumor progression. Although we cannot rule out *in vitro* proteolytic processing of Dsg2 during tissue prepping, we immunoblotted the same samples for Dsg1 showing the lack of processing of Dsg1 in these same tumor

samples. If there was *in vitro* processing, we suspect that Dsg1 would also be degraded similar to Dsg2. We note here that due to lack of spontaneous tumors in WT mice, we were unable to assess the endogenous level of Dsg2.

Discussion

During malignant transformation, cell-cell contacts are often reorganized, and desmosome assembly and stability are altered. However, there is conflicting evidence as to what roles desmosomal adhesion and/or desmosomal components play during cancer development and progression. We recently showed a correlation between Dsg2 expression and skin tumor progression, where upon we observed aberrant localization of Dsg2 in the cytoplasm and nuclei (Brennan and Mahoney, 2009). In the present study, we demonstrate co-localization of Dsg2 with Cav-1, which may have implications in the role of Dsg2 in carcinogenesis. We show that Dsg2 contains the necessary consensus-binding motifs to interact directly with the Cav-1 scaffolding domain. We believe that defining the interaction between Dsg2 and Cav-1 is important, since it may have an impact on cell adhesion (through regulation of turnover/dynamics), and possibly signaling, both of which could contribute to tumor progression.

We propose the following model of desmosome homeostasis (Figure 9) whereby desmosomes actively undergo assembly and disassembly. Junctional proteins such as desmogleins are subjected to dynamic turnover through a caveolae/lipid raft-dependent pathway. We show here that Dsg2 is proteolytically processed; resulting in a 95 kDa ectodomain shed product and a 65 kDa membrane-spanning fragment. The full-length and the truncated intracellular Dsg2 fragment associate with Cav-1 and are mobilized into membrane lipid rafts, where they are most likely fated for internalization and degradation. Altering the Dsg2-Cav-1 interaction, either by disrupting caveolae/lipid raft formation or with Cav-1 specific inhibitor peptides, leads to the retention of the 65 kDa fragment (Figure 5). We speculate that accumulation of this truncated Dsg2 fragment may disturb desmosome assembly and disrupt cell-cell adhesion.

The loss of cell-cell adhesion observed in our study is reminiscent of that reported using transgenic mice expressing NH2-terminally truncated Dsg3, which resulted in an accumulation of Dsg3DN, and disrupted desmosome assembly (Allen et al., 1996). If proteolytic processing and endocytic turnover of desmogleins are important for maintenance of desmosome dynamics, then results from studies using chimeric proteins, such as E-cadherin with Dsg3 (Andl and Stanley, 2001) or connexin with Dsg1 (Troyanovsky et al., 1993), may also reflect the loss of appropriate ectodomain shedding and desmoglein recycling.

Dsg2 was recently identified as a proteolytic target of ADAM17 (Bech-Serra *et al.*, 2006; Klessner *et al.*, 2009; Santiago-Josefat *et al.*, 2007), a member of the sheddase family. ADAMs are a class of enzymes involved in the ectodomain shedding of transmembrane proteins involved in receptor activation (Kenny and Bissell, 2007). ADAM17 cleaves Dsg2 in the region adjacent to the transmembrane domain, which would result in a shed ectodomain of approximately 95 kDa and an intracellular product of approximately 65 kDa. We believe the 65 kDa Dsg2 fragment is membrane-spanning, as we show that: (1)

antibodies recognizing extracellular epitopes detected this 95 kDa band, while antibodies raised against intracellular epitopes recognized the 65 kDa fragment and (2) our polyclonal antibody Ab10, raised against the extracellular membrane-anchoring (EC5) domain, detected both the shed ectodomain and the membrane-bound fragment. Thus, if the cleavage site is within the EC5 domain, then Ab10 may contain antibodies recognizing the shed ectodomain, as well as antibodies to the membrane spanning cytoplasmic domain.

Further supporting our hypothesis on the importance of Dsg2 proteolytic processing, in epithelial cancers EGFR is often deregulated, and inhibition of EGFR function promotes Dsg2 assembly into desmosomes (Lorch et al., 2007). Furthermore, this inhibition is at least in part through attenuation of ADAM-dependent cleavage of Dsg2, the latter of which contributes to its endocytic turnover (Klessner *et al.*, 2009). At the onset of apoptosis in intestinal epithelial cells, Dsg2 is cleaved by cysteine proteases, and down-regulation of Dsg2 by siRNA protects cells from apoptosis (Nava et al., 2007). Dsg2 has also been identified as a proteolytic target of caspase 3 (Cirillo et al., 2008), one of many caspases that comprise a family of proteins known to play critical roles in maintaining the cellular homeostasis between growth/survival and apoptosis (Denault and Salvesen, 2008; Rupinder et al., 2007). As mentioned above, ADAM17 is involved in the proteolytic processing of Dsg2. ADAM17 has been implicated in the development of cancer, and is being investigated as a possible target for anti-cancer therapies (Arribas et al., 2006). We are currently investigating the biological activity of the shed extracellular domain of Dsg2.

We previously reported that Dsg2 modulates cell growth and survival signaling pathways by demonstrating that ectopic expression of Dsg2 enhances epidermal proliferation and also increases susceptibility to two-step chemical-induced skin carcinogenesis (Brennan et al., 2007). In this report, we demonstrate enhanced expression and proteolytic processing of Dsg2 during skin tumor progression, which may contribute to the malignant phenotype, possibly through a caveolin-mediated pathway. This is a significant finding, as Cav-1 expression has been linked to many epithelial-derived cancers, and it has been shown that a loss of Cav-1 function plays a significant role in tumor initiation. It is proposed that Cav-1 binds to and inhibits kinases involved in mitogenic signaling pathways (Lajoie and Nabi, 2010). In many cancers, caveolins are downregulated and the loss of caveolae may release these signaling molecules to activate mitogenic pathways. Interestingly, *Cav-1* knockout mice display normal skin morphology, suggesting that, in addition to caveolin ablation, these mice may require an appropriate “oncogenic” stimulus. We propose that during skin tumor development, the up-regulation of an oncogenic stimulus such as Dsg2 and the concomitant down-regulation of caveolins may provide the necessary stimuli for cell proliferation, signaling activation and malignant transformation. Furthermore, down-regulation of caveolins may result in accumulation of the truncated Dsg2 fragment, which could potentially disrupt cell-cell adhesion, a process crucial for tumor cell migration and egression.

Materials and Methods

Antibodies

Antibodies from our laboratories were Ab10 (1:10000 IB), 6D8 (1:10 IF and 1:100 IB), 10D2 (1:10 IF and 1:100 IB), 6F9 β-catenin 1:1000 IB and 11E4 γ-catenin (1:500 IB). Commercially purchased primary antibodies were: Cav-1 (1:200 immunofluorescence (IF), 1:1000 immunoblotting (IB)) and H-145 (1:1000 IB) from Santa Cruz Biotechnology (Santa Cruz, CA, USA); E-cadherin (1:2500 IB), Cav-2 (1:1000 IB), Flotillin 1 (1:500 IB) and Flotillin 2 (1:5000 IB) from BD Transduction Labs (Franklin Lakes, NJ, USA); Flag M2 (1:1000 IF and 1:1000 IB) and Flag pAb (1:1000 IB) were from Sigma, (St. Louis, MO), USA; DG3.10 (1:200 IF and 1:1000 IB) from RDI Corp (Henderson, NV, USA); β-actin (1:100000 IB) from Calbiochem, San Diego, CA, USA); and GST (1:2500 IB) from GE Healthcare (Piscataway, NJ, USA). Secondary antibodies included: Alexa Flor 594- and Alexa Flor 488-conjugated (1:400, Molecular probes, Eugene, OR, USA) and HRP-conjugated (1:5000, Jackson labs, Bar Harbor, Maine, USA).

GST fusion proteins

cDNA encoding the intracellular domains of Dsg1 (1921-3845) and Dsg2 (1911-3516) were generated by PCR and inserted by in-frame cloning into the vector PGEX4T-1 (GE Healthcare) at *Bam*HI and *Sal*I restriction sites for Dsg1 and at *Bam*HI and *Not*I restriction sites for Dsg2. GST fusion proteins were produced in BL21 *Escherichia coli* cells after induction with isopropyl-β-D-thiogalactoside (1 mM) and purified as previously described in detail (Brennan and Mahoney, 2009).

Cell culture, drug treatment and protein extraction

A431, HaCaT and JAR cells (ATCC, Manassas, VA, USA) were cultured in DMEM medium supplemented with penicillin/streptomycin and 10% fetal bovine serum (FBS). To detect shedding of the Dsg2 ectodomain, medium was collected after 2 days in DMEM without FBS and concentrated by 10 fold using Amicon Ultra concentrators (Millipore Corp, Billerica, MA, USA). To enhance shedding, A431 cells were treated with camptothecin (10 mM) in serum free medium for 5-6 hrs. Cells were lysed in Laemmli buffer. For Tx-soluble proteins, cells were incubated on ice for 20 min in a 1% Tx-containing buffer (50 mM Tris-HCl (pH 7.5), 150 mM NaCl, and 5 mM EDTA), complete with protease inhibitors (Roche Diagnostics, Indianapolis, IN, USA) and phosphatase inhibitors (Sigma). The insoluble pellet was resuspended in Laemmli buffer for Tx-insoluble proteins.

To disrupt lipid microdomains, cells were treated with methyl-β-cyclodextrin (MβCD, 10 mM) or filipin (5 μg/ml) (Sigma). MβCD and filipin have been extensively used as the standard methods to disrupt raft-like microdomains. We are aware that there are limitations to the use of MβCD because it may affect both caveolin levels and caveolae structures and may target both caveolar and non-caveolar rafts. However, the key point is that Dsg2 can be localized to lipid rafts and can interact with caveolins.

Dispase-based keratinocyte dissociation assay

A431 cells were grown in 6-well culture dishes to confluency in DMEM + 10% FCS and then treated with 5 μM AP or AP-Cav-1 peptides in serum-free medium for 2 hr. Cells were washed with HBSS and incubated with dispase I (BD Biosciences, San Diego, CA) for 20-30 min. The lifted cell sheets were subjected to dispase-based dissociation assay by pipetting 5 times using a 1-ml pipet. Cell fragments were fixed in 10% formalin solution and stained with crystal violet.

Immunoblotting, immunohistochemistry and immunoprecipitation

Immunoblotting was performed with 2-25 μg of protein in each lane resolved over 5 or 12% SDS-PAGE (Bio-Rad Labs, Hercules, CA, USA) as previously described in detail (Brennan et al., 2007). Signals were detected by chemiluminescence (ECL; GE Healthcare). For Western blotting of biotinylated AP and AP-Cav-1 peptides, immunoprecipated proteins were resolved over a 20% SDS-PAGE Tricine gel (BioRad Labs) and electrotransferred for 30 min at a constant 80 V to a polyvinylidene difluoride (PVDF) membrane. Non-specific sites were blocked in Superblock (Thermo Scientific, Waltham, MA, USA), membranes were then incubated with strep-avidin HRP (1:1000, Thermo Scientific) and the immunoreactive bands visualized by chemiluminescence.

For immunofluorescence, OCT-fixed human skin sections (5 μm) were prepared as previously described (Brennan et al., 2007). Briefly, tissue sections were fixed in 100% methanol and permeabilized in 1% Tx in PBS. Nuclei were stained with DAPI (Sigma) prior to mounting for viewing. Similar steps were performed for immunostaining of cultured cells. Fluorescent images were acquired using a Hamamatsu monochromatic digital camera (Phase 3 Imaging Systems, Glen Mills, PA, USA; C4742-95), and analyzed using Image Pro 6.1 imaging software (Media Cybernetics, Bethesda, MD, USA). Confocal images were obtained using a Zeiss LSM 510 META confocal scanning microscropic system and software (Bioimaging Facility, Thomas Jefferson University, Philadelphia, PA, USA).

For immunoprecipitation, cells were solubilized in a buffer containing 50 mM Tris HCl (pH 7.5), 150 mM NaCl, 5 mM EDTA, 1% Tx, 1 mM PMSF and protease and phosphatase inhibitors. Samples were pre-cleared with mouse or rabbit IgG Agarose (25 μl; Sigma). Lysates were then incubated in antibodies (0.3 ml 6D8 or 5 μg/ml anti-Cav-1) and protein A/G Agarose (30 μl, Pierce Biotechnology). Immune complexes were washed with 1%Tx-PBS and suspended in Laemmli buffer for immunoblotting.

Isolation of caveolin-rich membrane fractions

Cells were washed twice with ice-cold PBS and scraped into TNE buffer (25 mM Tris-HCl (pH 7.5), 150 mM NaCl and 5 mM EDTA) containing 1% Tx, PMSF, protease and phosphatase inhibitors (Galbiati et al., 2000). Cells were disrupted using a loose-fitting Dounce Homogenizer (20 strokes), and sucrose concentration was brought to 45% by mixing 2 ml of cell lysates with equal volume of 90% sucrose. The mixture was placed at the bottom of an ultracentrifuge tube, and a discontinuous sucrose gradient was formed above the cell mixture by over-laying 4 ml each of 35% and 5% sucrose. The samples were

centrifuged at 40000 rpm for 16–20 h in a SW41 rotor (Beckman Instruments, Fullerton, CA). Twelve 1 ml fractions were collected from the top.

Skin tumor induction and tissue extraction

We recently established transgenic mice expressing Dsg2 in the differentiating layers of the epidermis under control of the involucrin (Inv) promoter (Inv-Dsg2) (Brennan et al., 2007). Briefly the mouse *Dsg2-Flag* cDNA was subcloned into the pH3700-pL2 parental vector epitope at the *Not*I restriction site downstream of the involucrin promoter. The genotyping and characterization of the transgenic mice was previously described in detail (Brennan et al., 2007). Adult wild-type and Inv-Dsg2 transgenic mice (6- to 8-weeks old) were treated once with DMBA (400 nmol in 200 µl acetone) followed by TPA (17 nmol in 200 µl acetone) twice weekly, as previously described (Brennan et al., 2007). Mouse back skin and tumors were processed in RIPA buffer (50 mM Tris-HCl (pH 7.5), 150 mM NaCl, 1% Nonidet P-40, 0.5% deoxycholate, 0.1% SDS and protease inhibitors).

Supplementary Material

Refer to Web version on PubMed Central for supplementary material.

Acknowledgments

We thank Dr. Abhilasha Gupta for critically reading this paper and her insightful discussions. This work was supported by grants from the National Institutes of Health to M. Mahoney (R01 AR47938), J. Wahl (R01 DE01905) and K. Green (R01 CA122151).

References

Allen E, Yu QC, Fuchs E. Mice expressing a mutant desmosomal cadherin exhibit abnormalities in desmosomes, proliferation, and the epidermal differentiation. J Cell biol. 1996; 133:1367–1382. [PubMed: 8682871]

Andl CD, Stanley JR. Central role of the plakoglobin-binding domain for desmoglein 3 incorporation into desmosomes. J Invest Dermatol. 2001; 117:1068–1074. [PubMed: 11710914]

Arribas J, Bech-Serra JJ, Santiago-Josefat B. ADAMs, cell migration and cancer. Cancer Metastasis Rev. 2006; 25:57–68. [PubMed: 16680572]

Bech-Serra JJ, Santiago-Josefat B, Esselens C, Saftig P, Baselga J, Arribas J, et al. Proteomic identification of desmoglein 2 and activated leukocyte cell adhesion molecule as substrates of ADAM17 and ADAM10 by difference gel electrophoresis. Mol Cell Biol. 2006; 26:5086–5095. [PubMed: 16782893]

Biedermann K, Vogelsang H, Becker I, Plaschke S, Siewert JR, Hofler H, et al. Desmoglein 2 is expressed abnormally rather than mutated in familial and sporadic gastric cancer. J Pathol. 2005; 207:199–206. [PubMed: 16025435]

Brennan D, Hu Y, Joubeh S, Choi YW, Whitaker-Menezes D, O'Brien T, et al. Suprabasal Dsg2 expression in transgenic mouse skin confers a hyperproliferative and apoptosis-resistant phenotype to keratinocytes. J Cell Sci. 2007; 120:758–771. [PubMed: 17284515]

Brennan D, Mahoney MG. Increased expression of Dsg2 in malignant skin carcinomas: A tissue-microarray based study. Cell Adh Migr. 2009; 3:148–154. [PubMed: 19458482]

Brown DA, London E. Functions of lipid rafts in biological membranes. Annu Rev Cell Dev Biol. 1998; 14:111–136. [PubMed: 9891780]

Capozza F, Williams TM, Schubert W, McClain S, Bouzahzah B, Sotgia F, et al. Absence of caveolin-1 sensitizes mouse skin to carcinogen-induced epidermal hyperplasia and tumor formation. Am J Pathol. 2003; 162:2029–2039. [PubMed: 12759258]

Chen ST, Lin SY, Yeh KT, Kuo SJ, Chan WL, Chu YP, et al. Mutational, epigenetic and expressional analyses of caveolin-1 gene in breast cancers. Int J Mol Med. 2004; 14:577–582. [PubMed: 15375584]

Cheng X, Koch PJ. In vivo function of desmosomes. J Dermatol. 2004; 31:171–187. [PubMed: 15187337]

Cirillo N, Lanza M, De Rosa A, Cammarota M, La Gatta A, Gombos F, et al. The most widespread desmosomal cadherin, desmoglein 2, is a novel target of caspase 3-mediated apoptotic machinery. J Cell Biochem. 2008; 103:598–606. [PubMed: 17559062]

Del Galdo F, Lisanti MP, Jimenez SA. Caveolin-1, transforming growth factor-beta receptor internalization, and the pathogenesis of systemic sclerosis. Curr Opin Rheumatol. 2008; 20:713–719. [PubMed: 18949888]

Delva E, Jennings JM, Calkins CC, Kottke MD, Faundez V, Kowalczyk AP. Pemphigus vulgaris IgG-induced desmoglein-3 endocytosis and desmosomal disassembly are mediated by a clathrin- and dynamin-independent mechanism. J Biol Chem. 2008; 283:18303–18313. [PubMed: 18434319]

Denault JB, Salvesen GS. Apoptotic caspase activation and activity. Methods Mol Biol. 2008; 414:191–220. [PubMed: 18175821]

Denning MF, Guy SG, Ellerbroek SM, Norvell SM, Kowalczyk AP, Green KJ. The expression of desmoglein isoforms in cultured human keratinocytes is regulated by calcium, serum, and protein kinase C. Exp Cell Res. 1998; 239:50–59. [PubMed: 9511724]

Engelman JA, W CC, Yasuhara S, Song KS, Okamoto T, Lisanti MP. Recombinant expression of caveolin-1 in oncogenically transformed cells abrogates anchorage-independent growth. J Biol Chem. 1997; 272:16374–16381. [PubMed: 9195944]

Eshkind L, Tian Q, Schmidt A, Franke WW, Windoffer R, Leube RE. Loss of desmoglein 2 suggests essential functions for early embryonic development and proliferation of embryonal stem cells. Eur J Cell Biol. 2002; 81:592–598. [PubMed: 12494996]

Fielding PE, Fielding CJ. Plasma membrane caveolae mediate the efflux of cellular free cholesterol. Biochemistry. 1995; 34:14288–14292. [PubMed: 7578031]

Fra AM, Williamson E, Simons K, Parton RG. Detergent-insoluble glycolipid microdomains in lymphocytes in the absence of caveolae. J Biol Chem. 1994; 269:30745–20748. [PubMed: 7982998]

Furuchi T, Anderson RG. Cholesterol depletion of caveolae causes hyperactivation of extracellular signal-related kinase (ERK). J Biol Chem. 1998; 273:21099–21104. [PubMed: 9694863]

Galbiati F, Volonte D, Brown AM, Weinstein DE, Ben-Ze'ev A, Pestell RG, et al. Caveolin-1 expression inhibits Wnt/beta-catenin/Lef-1 signaling by recruiting beta-catenin to caveolae membrane domains. J Biol Chem. 2000; 275:23368–23377. [PubMed: 10816572]

Garrod DR, Merritt AJ, Nie Z. Desmosomal cadherins. Curr Opin Cell Biol. 2002; 14:537–545. [PubMed: 12231347]

Gassmann MG, Werner S. Caveolin-1 and -2 expression is differentially regulated in cultured keratinocytes and within the regenerating epidermis of cutaneous wounds. Exp Cell Res. 2000; 258:23–32. [PubMed: 10912784]

Harada H, Iwatsuki K, Ohtsuka M, Han G, Kaneko F. Abnormal desmoglein expression by squamous cell carinoma cells. Acta Derm Venereol. 1996; 16:417–420. [PubMed: 8982400]

Keim SA, Johnson KR, Wheelock MJ, Wahl JK. Generation and characterization of monoclonal antibodies against the proregion of human desmoglein-2. Hybridoma. 2008; 27:249–258. [PubMed: 18707543]

Kenny PA, Bissell MJ. Targeting TACE-dependent EGFR ligand shedding in breast cancer. J Clin Invest. 2007; 117:337–345. [PubMed: 17218988]

Klessner JL, Desai BV, Amargo EV, Getsios S, Green KJ. EGFR and ADAMs cooperate to regulate shedding and endocytic trafficking of the desmosomal cadherin desmoglein 2. Mol Biol Cell. 2009; 20:328–337. [PubMed: 18987342]

Kurzchalia TV, Parton RG. Membrane microdomains and caveolae. Curr Opin Cell Biol. 1999; 11:424–431. [PubMed: 10449327]

Kurzen H, Munzing I, Hartschuh W. Expression of desmosomal proteins in squamous cell carcinomas of the skin. J Cutan Pathol. 2003; 30:621–630. [PubMed: 14744087]

Lajoie P, Nabi IR. Lipid rafts, caveolae, and their endocytosis. Int Rev Cell Mol Biol. 2010; 282:135–63. [PubMed: 20630468]

Lee SW, Reimer CL, Oh P, Campbell DB, Schnitzer JE. Tumor cell growth inhibition by caveolin re-expression in human breast cancer cells. Oncogene. 1998; 16:1391–1397. [PubMed: 9525738]

Lisanti MP, S PE, Tang Z, Sargiacomo M. Caveolae, caveolin and caveolin-rich membrane domains: a signalling hypothesis. Trends Cell Biol. 1994; 4:231–235. [PubMed: 14731661]

Lorch JH, Thomas TO, Schmoll HJ. Bortezomib inhibits cell-cell adhesion and cell migration and enhances epidermal growth factor receptor inhibitor-induced cell death in squamous cell cancer. Cancer Res. 2007; 67:727–734. [PubMed: 17234784]

Mahoney MG, Hu Y, Brennan D, Bazzi H, Christiano AM, Wahl JKr. Delineation of diversified desmoglein distribution in stratified squamous epithelia: implications in diseases. Exp Dermatol. 2006; 15:101–109. [PubMed: 16433681]

Mahoney MG, Simpson A, Aho S, Uitto J, Pulkkinen L. Interspecies conservation and differential expression of mouse desmoglein gene family. Exp Derm. 2002; 11:115–125. [PubMed: 11994138]

Nava P, Laukoetter MG, Hopkins AM, Laur O, Gerner-Smidt K, Green KJ, et al. Desmoglein-2: a novel regulator of apoptosis in the intestinal epithelium. Mol Biol Cell. 2007; 18:4565–4578. [PubMed: 17804817]

Okamoto CT. Endocytosis and transcytosis. Adv Drug Deliv Rev. 1998; 29:215–228. [PubMed: 10837591]

Okamoto T, Schlegel A, Scherer PE, Lisanti MP. Caveolins, a family of scaffolding proteins for organizing “preassembled signaling complexes” at the plasma membrane. J Biol Chem. 1998; 273:5419–5422. [PubMed: 9488658]

Orlichenko L, Huang B, Krueger E, McNiven MA. Epithelial growth factor-induced phosphorylation of caveolin 1 at tyrosine 14 stimulates caveolae formation in epithelial cells. J Biol Chem. 2006; 281:4570–4579. [PubMed: 16332692]

Park DS, Lee H, Frank PG, Razani B, Nguyen AV, Parlow AF, et al. Caveolin-1-deficient mice show accelerated mammary gland development during pregnancy, premature lactation, and hyperactivation of the Jak-2/STAT5a signaling cascade. Mol Biol Cell. 2002; 13:3416–30. [PubMed: 12388746]

Rupinder SK, Gurpreet AK, Manjeet S. Cell suicide and caspases. Vascul Pharmacol. 2007; 46:383–393. [PubMed: 17382599]

Santiago-Josefat B, Esselens C, Bech-Serra JJ, Arribas J. Post-transcriptional up-regulation of ADAM17 upon epidermal growth factor receptor activation and in breast tumors. J Biol Chem. 2007; 282:8325–8331. [PubMed: 17227756]

Schäfer S, Koch PJ, Franke WW. Identification of the ubiquitous human desmoglein, Dsg2, and the expression catalogue of the desmoglein subfamily of desmosomal cadherins. Exp Cell Res. 1994; 211:391–399. [PubMed: 8143788]

Scherer PE, Tang ZL, Chun M, Sargiacomo M, Lodish HF, Lisanti MP. Caveolin isoforms differ in their N-terminal protein sequence and subcellular distribution. J Biol Chem. 1995; 270:16395–16401. [PubMed: 7608210]

Schnitzer JE, Oh P. Aquaporin-1 in plasma membrane and caveolae provides mercury-sensitive water channels across lung endothelium. Am J Physiol. 1996; 270:H416–22. [PubMed: 8769778]

Sedding DG, Hermsen J, Seay U, Eickelberg O, Kummer W, Schwencke C, et al. Caveolin-1 facilitates mechanosensitive protein kinase B (Akt) signaling in vitro and in vivo. Circ Res. 2005; 96:635–642. [PubMed: 15731459]

Severs NJ. Caveolae: static inpocketings of the plasma membrane, dynamic vesicles or plain artifact? J Cell Sci. 1988; 90:341–348. [PubMed: 3075612]

Shaul PW, Anderson RG. Role of plasmalemmal caveolae in signal transduction. Am J Physiol. 1998; 275:L843–51. [PubMed: 9815100]

Simons K, Ikonen E. Functional rafts in cell membranes. Nature. 1997; 387:569–572. [PubMed: 9177342]

Simons K, Toomre D. Lipid rafts and signal transduction. Nat Rev Mol Cell Biol. 2000; 1:31–39. [PubMed: 11413487]

Singer SJ, Nicolson GL. The fluid mosaic model of the structure of cell membranes. Science. 1972; 175:720–731. [PubMed: 4333397]

Smart EJ, Ying Y, Donzell WC, Anderson RG. A role for caveolin in transport of cholesterol from endoplasmic reticulum to plasma membrane. J Biol Chem. 1996; 271:29427–29435. [PubMed: 8910609]

Song J, Dohlman HG. Partial constitutive activation of pheromone responses by a palmitoylation-site mutant of a G protein alpha subunit in yeast. Biochemistry. 1996; 35:14806–14817. [PubMed: 8942643]

Tang Z, Scherer PE, Okamoto T, Song KS, Chu C, Kohtz DS, et al. Molecular cloning of caveolin-3, a novel member of the caveolin gene family expressed predominantly in muscle. J Biol Chem. 1996; 271:2255–2261. [PubMed: 8567687]

Trojan L, Schaaf A, Steidler A, Haak M, Thalmann G, Knoll T, et al. Identification of metastasis-associated genes in prostate cancer by genetic profiling of human prostate cancer cell lines. Anticancer Res. 2005; 25:183–191. [PubMed: 15816537]

Troyanovsky SM, Eshkind LG, Troyanvsky RB, Leube RE, Franke WW. Contributions of cytoplasmic domains of desmosomal cadherins to desmosome assembly and intermediate filament anchorage. Cell. 1993; 72:561–574. [PubMed: 7679953]

Wang PY, Liu P, Weng J, Sontag E, Anderson RG. A cholesterol-regulated PP2A/HePTP complex with dual specificity ERK1/2 phosphatase activity. EMBO J. 2003; 22:2658–2667. [PubMed: 12773382]

Whittock NV. Genomic sequence analysis of the mouse desmoglein cluster reveals evidence for six distinct genes: characterization of mouse DSG4, DSG5, and DSG6. J Invest Dermatol. 2003; 120:970–980. [PubMed: 12787123]

Zheng X, Ray S, Bollag WB. Modulation of phospholipase D-mediated phosphatidylglycerol formation by differentiating agents in primary mouse epidermal keratinocytes. Biochim Biophys Acta. 2003; 1643:25–36. [PubMed: 14654225]

Abbreviations

AP	antennapedia peptide
Dsg2	desmoglein 2
Cav-1	caveolin-1
GST	Gluthathione-S-transferase
MβCD	methyl β cyclodextran
Tx	Triton X-100

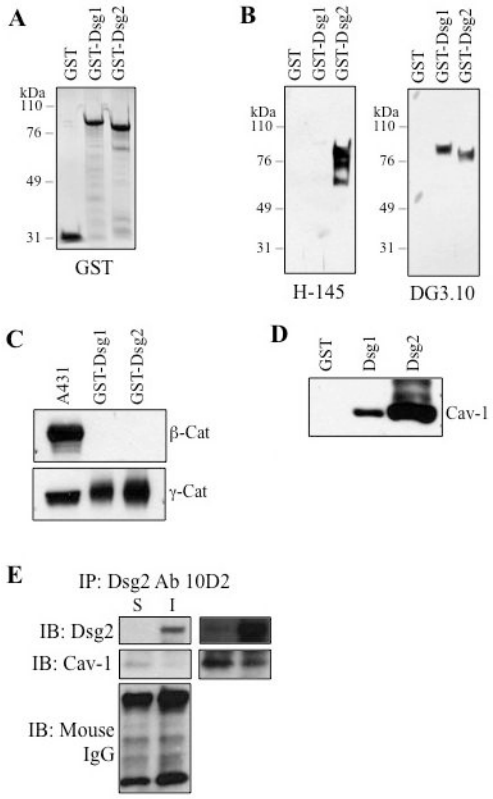

Figure 1.

Cav-1 is a binding partner of desmogleins. (**A**) Coomasie staining of purified GST and GST fusion proteins with intracellular domains of Dsg1 (GST-Dsg1) or Dsg2 (GST-Dsg2). (**B**) Immunoblotting of GST, GST-Dsg1 and GST-Dsg2 using antibodies H-145 and DG3.10. H-145 recognized Dsg2 only, while DG3.10 recognized both Dsg1 and Dsg2. (**C**) These fusion proteins were used in a GST pull-down assay with A431 cell lysates. While A431 cells expressed both γ-catenin and β-catenin, Dsg1 and Dsg2 were able to pull down γ-catenin but not β-catenin. (**D**) GST pull-down assay with GST, GST-Dsg1 and GST-Dsg2 and A431 cell lysates, followed by Western blotting for Cav-1. Cav-1 was detected in the pull-down with Dsg1 and Dsg2 but not GST. (**E**) Immunoprecipitation assay further confirms that Dsg2 binds to Cav-1. Tx-soluble (S) and -insoluble (I) proteins were extracted from A431 cells and subjected to immunoprecipitation for Dsg2 (antibody 10D2). The precipitated products were immunoblotted for Dsg2 (Ab H-145), Cav-1 and mouse IgG (for equal antibody loading). Panels to the right are overexposed. I, Tx-insoluble; Tx, Triton X-100; S, Tx-soluble.

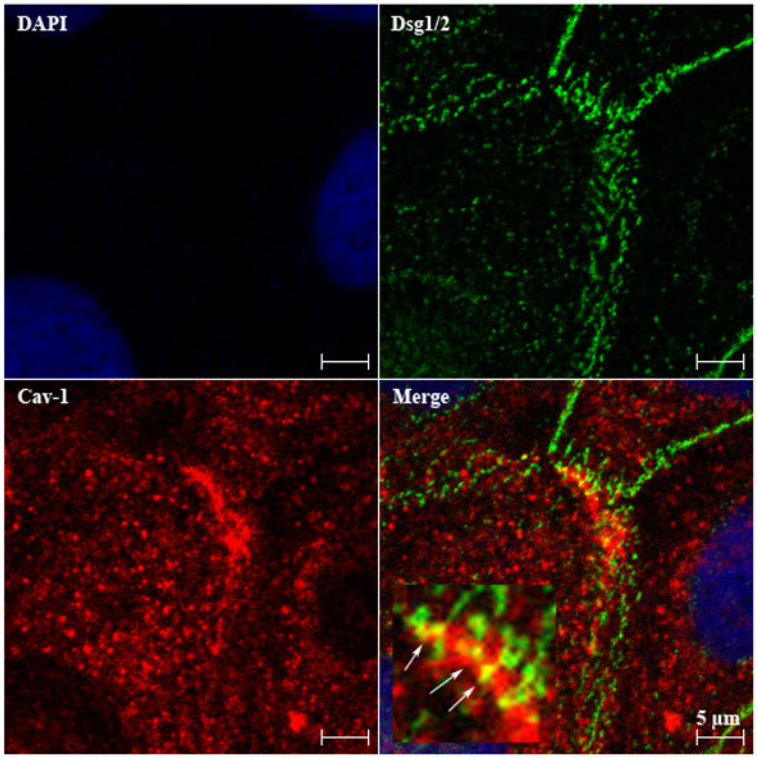

Figure 2.

Co-localization of Cav-1 and Dsg2 in epithelial cells. Cultured A431 cells were grown to confluency, fixed and stained for Dsg2 and Cav-1. Confocal microscopy showing co-localization of Dsg2 (green) and Cav-1 (red) in A431 cells. Inset shows higher resolution merged image of cell-cell border area and arrows demarcate double labeling (yellow) of Cav-1 and Dsg2. We note here that we used antibody DG3.10, which recognizes both Dsg1 and Dsg2, but since A431 cells do not express Dsg1, the observed staining is Dsg2 only.

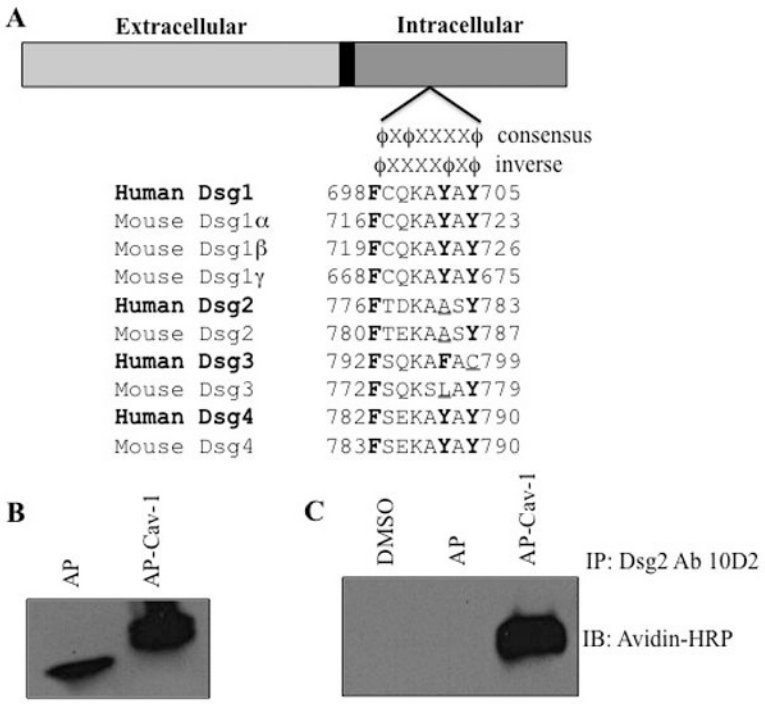

Figure 3.

Dsg2 associates with the Cav-1 consensus binding peptide. (**A**) Sequence analysis of Dsg1-4 showing putative Cav-1 binding sites in the inverse orientation of the consensus motif, φXφXXXXφ. φ, aromatic amino acids (F, Y and W); X, any amino acid. In bold are aromatic amino acids and underlined are hydrophobic amino acids. (**B**) A431 cells were incubated with the biotinylated antennapedia peptide (AP; [(biotin)-RQPKIWFPNRRKPWKK-(OH)]; 5 μM) or the Cav-1 consensus binding peptide conjugated to AP (AP-Cav-1; [(biotin)-RQPKIWFPNRRKPWKKDGIWKASFTTFTVTKYWFYR-(OH)]; 5 μM) for 2 hr. Cells were lyzed and extracted in a Tx lysis buffer, and proteins were resolved over SDS-PAGE and immunoblotted with Avidin-HRP to show incorporated biotinylated AP and AP-Cav-1. (**C**) Total extracted proteins were then subjected to immunoprecipitation with the Dsg2 antibody 10D2 and protein A/G agarose. Precipitated products were immunoblotted with HRP-strep avidin. The results show that Dsg2 associated with AP-Cav-1, but not AP alone.

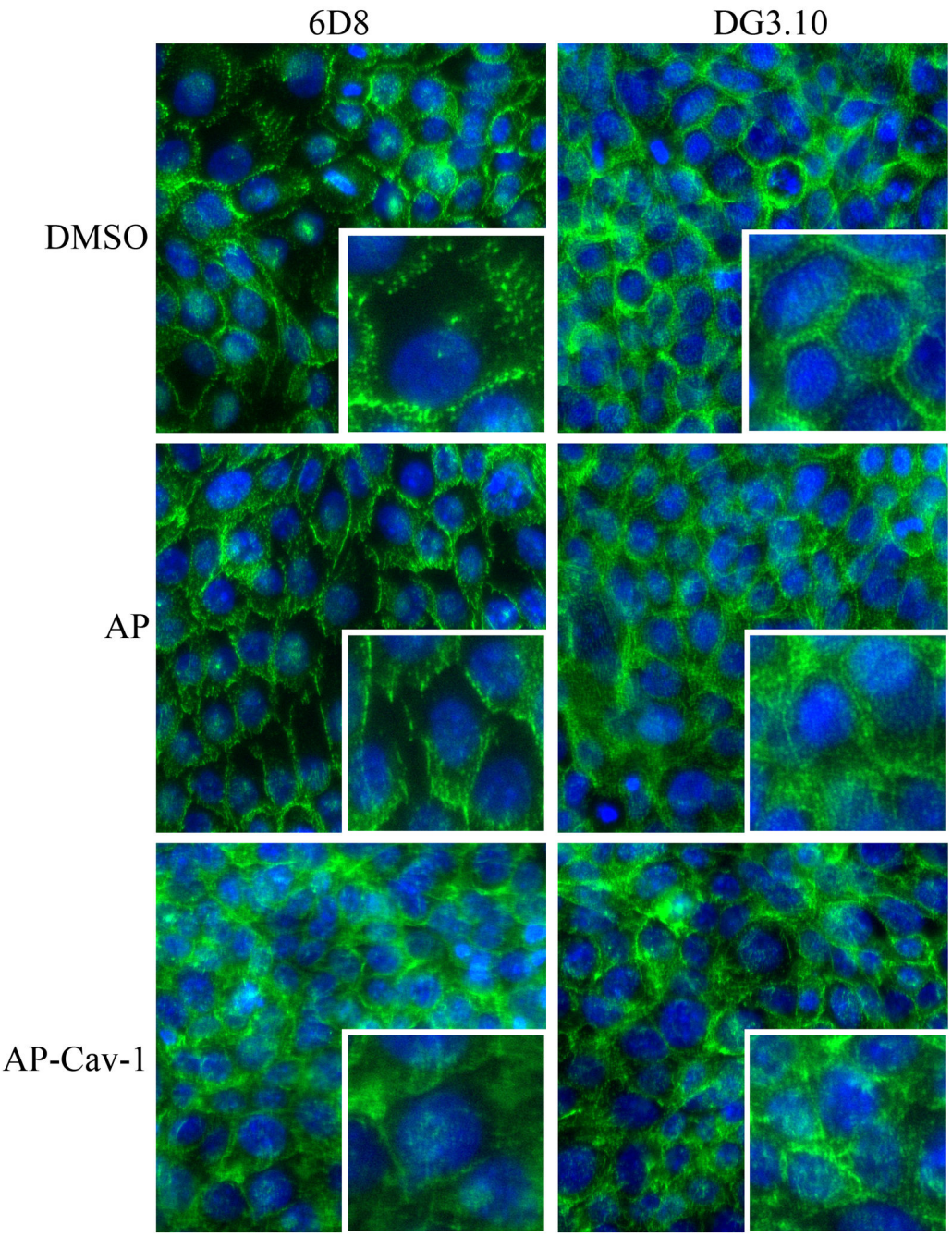

Figure 4.

Cav-1 consensus binding peptide perturbs membrane localization of Dsg2. Cells were treated with DMSO, AP peptide or AP-Cav-1 peptide for 24 hr. They were then washed, fixed and immunostained for Dsg2 (antibodies 6D8 and DG3.10). Insets: enlarged images. In response to AP-Cav1 peptide, but not DMSO or AP peptide alone, the staining for Dsg2 appeared more diffuse and less punctate at the cell-cell border. Nuclei counterstained with DAPI (blue).

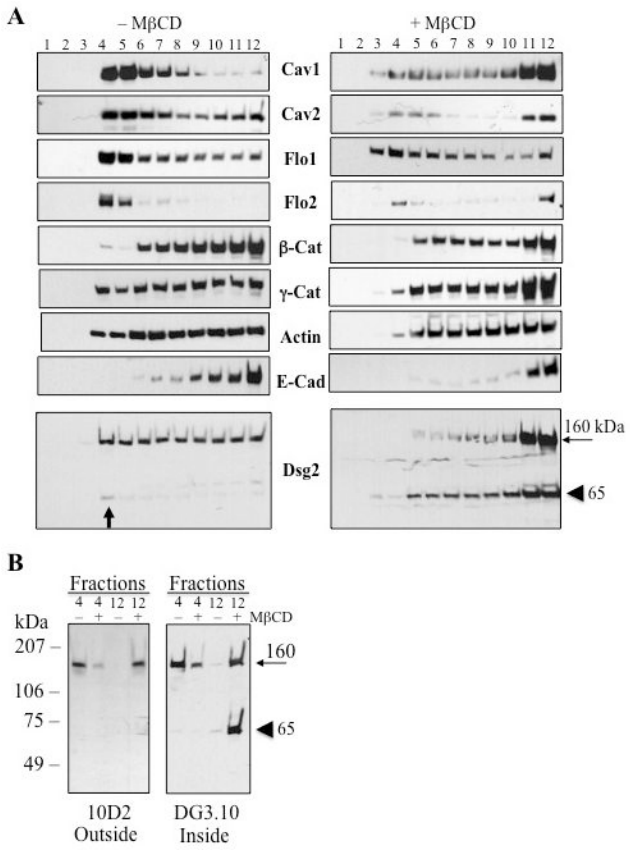

Figure 5.

Localization of Dsg2 and Cav-1 to membrane lipid rafts. (**A**) A431 cells were treated with MβCD (10 mM) for 1 hr and extracted in a Tris-NaCl-EDTA buffer containing Tx. Proteins were subjected to a discontinous (5-35%) sucrose-gradient separation, resolved over SDS-PAGE and immunoblotted for Cav-1, Cav-2, Flo1, Flo2, β-Cat, γ-Cat, actin, E-Cad and Dsg2. Immunoblotting revealed that Cav-1 localized predominantly to low-density fractions 4 and 5 (top left panel), corresponding to lipid rafts. Dsg2 was distributed through all fractions from 4-12. Treatment with MβCD (10 mM) for 1 hr, disrupted lipid rafts, and shifted both Cav-1 and Dsg2 to the more dense fractions. In addition to the 160 kDa Dsg2 full-length protein, we observed a 65 kDa band in the lipid raft fraction # 4 (vertical arrow). Accumulation of this fragment was enhanced and shifted to the denser fractions in the presence of MβCD (arrow head). We note that β-Cat, γ-Cat, E-Cad and actin fractioned to the lower, denser fractions, and remained relatively unchanged in the presence of MβCD. (**B**) Proteins from fractions 4 (lipid raft fraction) and 12 (high molecular weight, non-raft fraction) from above were resolved over SDS-PAGE and immunoblotted for Dsg2 using two different antibodies, 10D2 and DG3.10. Treatment with MβCD increased the level of the 65-kDa Dsg2 fragment as detected by DG3.10, but not 10D2.

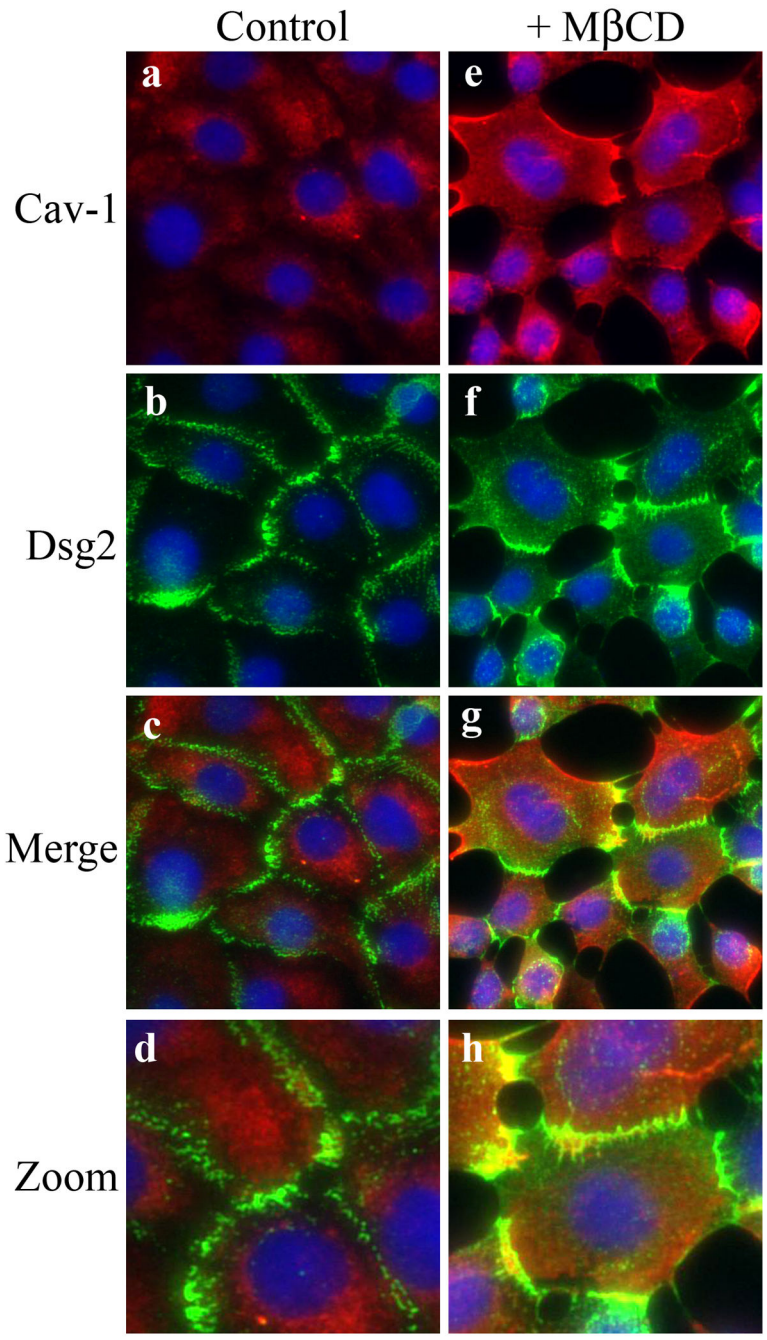

Figure 6.

Blocking of caveolae formation disrupts cell-cell adhesion. A431 cells were treated with MβCD (10 mM) for 1 hr, washed, fixed, and subjected to immunofluorescence staining for Dsg2 (green) and Cav-1 (red). Results show that blocking the formation of caveolae with MβCD resulted in partial loss of cell-cell adhesion and enhanced cytoplasmic staining of both Cav-1 and Dsg2. Nuclear staining with DAPI in blue.

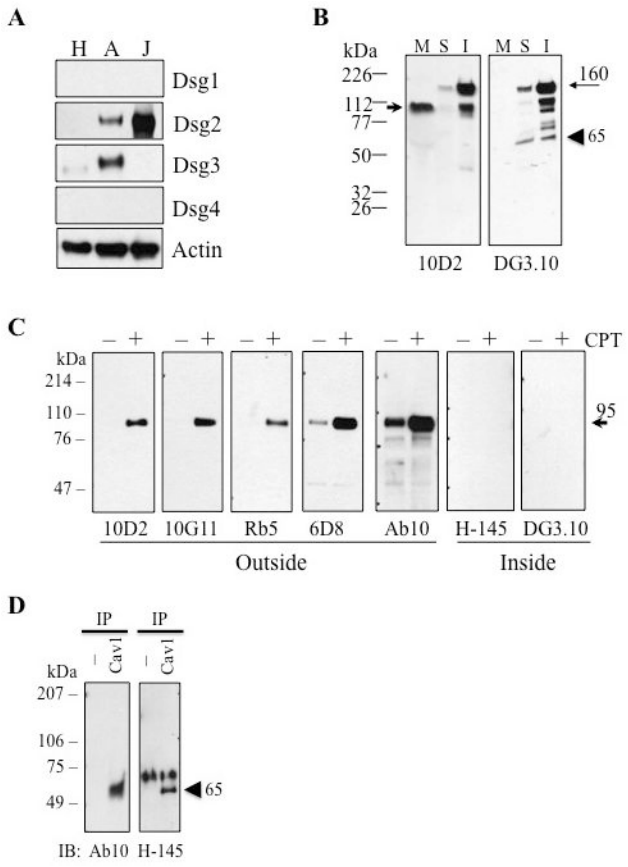

Figure 7.

Cav-1 associates with the processed 65 kDa Dsg2 fragment. (**A**) Cultured HaCaT (H), A431 (A) and JAR cells (J) were grown to confluency, lysed in Laemmli buffer and immunoblotted for Dsg1, Dsg2, Dsg3 and Dsg4. The blots were reprobed with Actin antibodies for equal loading. (**B**) Medium (M) was collected from JAR cells and concentrated. Cells were then extracted into Tx-soluble (S) and -insoluble (I) fractions. All protein fractions were processed for immunoblotting with 10D2 and DG3.10. A shed product of approximately 95 kDa was detected in the medium using 10D2 but not DG3.10. A 65-kDa product was detected in the Tx-soluble and –insoluble fractions with DG3.10, but not 10D2. (**C**) A431 cells were treated with camptothecin (5 μM) for 6 hr. Medium was collected, concentrated and immunoblotted to show enhanced Dsg2 ectodomain shedding as detected by antibodies to the ectodomain of Dsg2 (10D2, 10G11, Rb5, 6D8, and Ab10) but not antibodies to the cytoplasmic domain of Dsg2 (H-145 and DG3.10). (**D**) A431 cells were treated with camptothecin and then lysed in Tx lysis buffer. Cellular proteins were subjected to immunoprecipitation using Cav-1 antibodies and protein A/G agarose. Bound proteins were immunoblotted with the antibodies Ab10 and H-145 to show a protein of approximately 65 kDa recognized by the Dsg2 antibodies. CPT, camptothecin; I, Tx-insoluble; MβCD, methyl β cyclodextran; M, medium; S, Tx-soluble; Tx, Triton X-100.

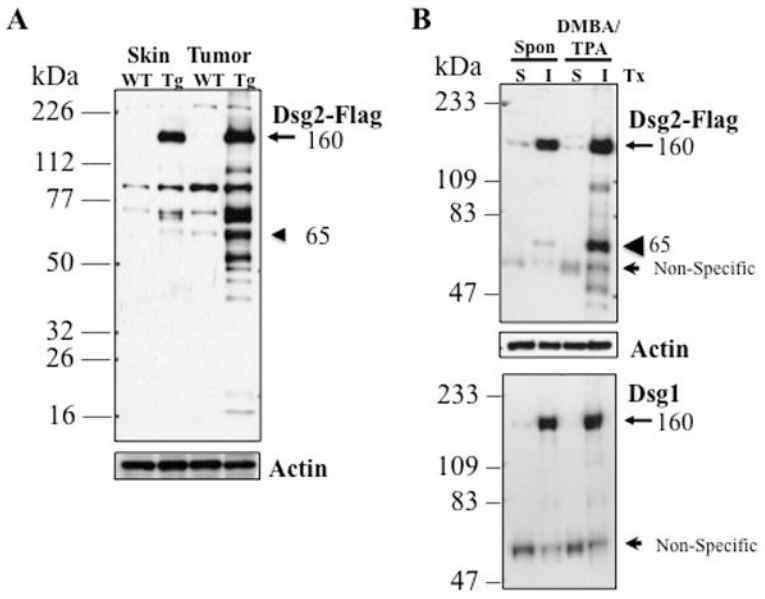

Figure 8.

Proteolytic processing of Dsg2 in skin tumors. (A) Representative examples of skin tumor developing in a wildtype (WT) and Inv-Dsg2 (Tg) mouse after 8 weeks of DMBA/TPA treatment. Tissues were lysed in Laemmli buffer and immunoblotted using Flag polyclonal antibody, showing multiple lower molecular weight protein fragments of Dsg2 in the Tg tumor. Unique bands estimated approximately in kDa: 160, 120, 100, 80, 75, 65, 55, 50, 45 and 40. Similar results were observed in two other sets of WT and Tg littermates. Blotting for Actin shows equal loading. (B) Proteolytic processing of Dsg2 was also observed in spontaneous tumors developed from aged Inv-Dsg2 Tg mice. DMBA/TPA-induced or spontaneously developed tumor tissues from Inv-Dsg2 transgenic mice were extracted in Tx lysis buffer. Tx-soluble and -insoluble proteins were resolved over SDS-PAGE and immunoblotted for Dsg2.Flag (monoclonal antibody), Dsg1 and Actin (for equal loading). The results show the presence of the 65 kDa Dsg2 fragment in the Tx–insoluble fractions of both spontaneous and chemical-induced skin tumors in Inv-Dsg2 Tg mice. The Dsg1 antibody only detected the full-length product of approximately 160 kDa. DMBA; 7,12-dimethyl-benz[a]anthracene; I, Tx-insoluble; S, Tx-soluble; Spon, spontaneous; TPA, phorbol ester 12-*O*-tetradecanoylphorbol-13 acetate; Tx, Triton X-100.

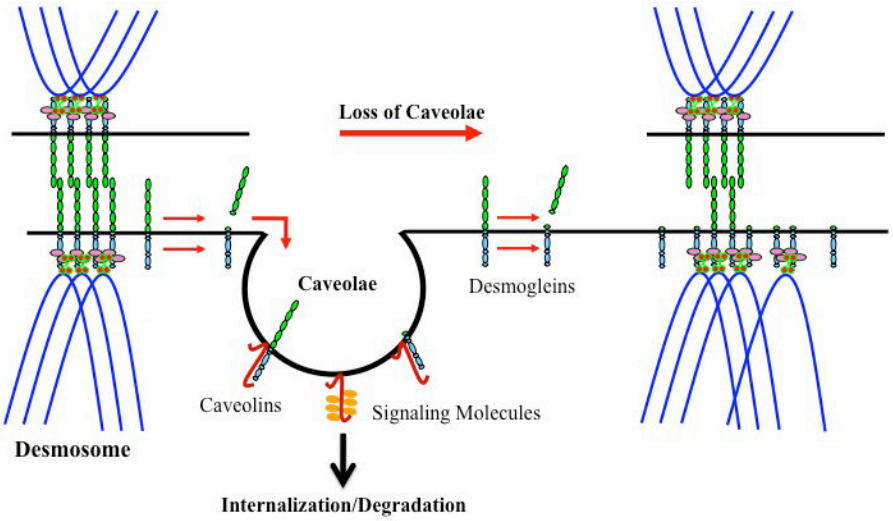

Figure 9.

Schematic diagram depicting the roles of Cav-1 and caveolae in desmoglein trafficking, and desmosome homeostasis. Full-length as well as cleaved desmogleins associate with Cav-1 in the caveolae, and are most likely fated for internalization and recycling. This model offers a mechanism by which desmogleins can be cleared from the plasma membrane and in the process possibly activate mitogenic cell signaling through their interaction with Cav-1. Loss of Cav-1 in cancer allows accumulation of the proteolytic fragments, which may affect cell-cell adhesion. Furthermore, loss of Cav-1 may also result in abnormal signaling.